Interorbital pairing and its physical consequences for iron pnictide superconductors

Yi Gao* and Wu-Pei Su
Department of Physics and Texas Center for Superconductivity, University of Houston, Houston, Texas 77204, USA

Jian-Xin Zhu
Theoretical Division, Los Alamos National Laboratory, Los Alamos, New Mexico 87545, USA

(Received 9 November 2009; revised manuscript received 4 January 2010; published 4 March 2010)

We study interorbital pairings of iron pnictide superconductors within a minimal two-orbital tight-binding model. We find that in real space, a set of self-consistently determined pairing order parameters forms two sublattices with a relative phase of π and the pairing symmetry is $d_{x^2-y^2} \sim \cos k_x - \cos k_y$. In momentum space, it corresponds to the η pairing proposed by Yang [Phys. Rev. Lett. **63**, 2144 (1989)], with nonzero momenta of Cooper pairs. One physical consequence of this type of pairing is the existence of a significant amount of zero energy (gapless) states around the Fermi surface even in the absence of disorder, which contradicts current experiments thus excluding such a pairing in iron pnictide superconductors.

DOI: 10.1103/PhysRevB.81.104504 PACS number(s): 74.20.Rp, 74.25.Dw, 74.81.−g

I. INTRODUCTION

The discovery of a new family of iron pnictide superconducting materials[1–6] has triggered a large effort in understanding the possible new mechanism of high-temperature superconductivity. Most of the parent compounds of iron pnictides have an antiferromagnetically ordered ground state,[7–10] which, upon doping, gives way to superconductivity. This behavior is similar to the cuprates. However, there is a growing consensus among researchers that Mott physics does not play a significant role for the iron pnictides, which remain itinerant for all doping levels, including parent compounds in which magnetic order is of spin-density-wave type rather than Heisenberg antiferromagnetism of localized spins.[11,12] As another contrast to the cuprates, electronic structure proposed by band-structure calculations[13–17] and supported by angle-resolved photoemission spectroscopy (ARPES) (Refs. 18–20) consists of multiple electron and hole sheets of Fermi surface, suggesting multiorbital physics is essential for superconductivity in the iron pnictides.[21]

So far, most of the theoretical works considering multiorbital superconductivity in the iron pnictides are based on Cooper pairing between electrons in the same orbit,[22–26] which corresponds to next-nearest-neighbor (nnn) intraorbital pairing in the 1-Fe/cell representation in real space. However, since the undoped iron pnictides are bad metals,[6,8] the typical Hubbard repulsion U between electrons should be in the intermediate regime. In this region, numerical studies have suggested that nearest-neighbor (nn) interorbital pairing transforming according to the B_{2g} representation of the lattice symmetry prevails.[27–30] Furthermore, the momenta of the Cooper pairs are presumed to be zero and thus excludes the possibility of spontaneous pairing inhomogeneity in real space, whose existence may enhance T_c and implicitly suggests the phenomenon of high critical temperature may rely on it.[31–33]

In this paper, we study a minimal two-orbital model with nearest-neighbor interorbital and next-nearest-neighbor intraorbital attractive interactions V_{nn} and V_{nnn}. By using Bogoliubov-de Gennes (BdG) equations, all the pairing order parameters are determined self-consistently and the phase diagram of the pairing symmetry is obtained. In the phase diagram where next-nearest-neighbor intraorbital pairing dominates, the pairing symmetry is $s_{x^2y^2} \sim \cos k_x \cos k_y$, consistent with that proposed by Mazin[16] and has been extensively discussed elsewhere[16,17,22,34] but when nearest-neighbor interorbital pairing prevails, we do not find the $s_{x^2+y^2} \sim \cos k_x + \cos k_y$ pairing symmetry as in Refs. 28–30, instead, the pairing order parameter forms two sublattices spontaneously with a relative phase of π and has $d_{x^2-y^2} \sim \cos k_x - \cos k_y$ symmetry, which has never been reported before. In momentum space, this type of pairing corresponds to the η pairing proposed by Yang,[35] with nonzero momenta of Cooper pairs. The dynamical spin susceptibility shows some agreement with neutron-scattering experiments while the calculated density of states (DOS) has a significant amount of zero energy (gapless) states around the Fermi surface even in the absence of disorder, which contradicts certain current experiments. However, whether interorbital pairing is possible or not still need to be verified by future experiments.

The outline of the paper is as follows: we lay down the model Hamiltonian and introduce the numerical method in Sec. II. The results and discussions are presented in Sec. III. The conclusion is given in Sec. IV.

II. METHODOLOGY

We begin with the minimal two-orbital model for the iron pnictides,[11] the Hamiltonian in real space can be written as

$$H = H_t + H_\Delta,$$

$$H_t = -\sum_{ij,\alpha\beta,\sigma} (t_{ij,\alpha\beta} + \mu\delta_{ij}\delta_{\alpha\beta}) c^\dagger_{i\alpha\sigma} c_{j\beta\sigma},$$

$$H_\Delta = \sum_{ij,\alpha\beta} (\Delta_{ij,\alpha\beta} c^\dagger_{i\alpha\uparrow} c^\dagger_{j\beta\downarrow} + \mathrm{H.c.}). \quad (1)$$

Here $c^\dagger_{i\alpha\sigma}$ creates an electron on site i in α orbital and with spin σ. Since we consider a two-orbital model, $\alpha = 1(2)$ rep-

resents d_{xz} (d_{yz}) orbital. The quantity $t_{ij,\alpha\beta}$ is the hopping integral from the β orbital on site j to the α orbital on site i and is given in Refs. 11 and 36 (also illustrated in Fig. 1). The quantity μ is the chemical potential. The pairing order parameter in real space is described by $\Delta_{ij,\alpha\beta} = V_{ij,\alpha\beta}\langle c_{j\beta\downarrow} c_{i\alpha\uparrow}\rangle$. In the present work, we only consider the spin singlet pairing. Hereafter, we assume there exist only nearest-neighbor interorbital and next-nearest-neighbor intraorbital pairing, so the attractive interaction $V_{ij,\alpha\beta}$ can be written as

$$V_{ij,\alpha\beta} = \begin{cases} V_{\mathrm{nn}} & \text{for } i,j \text{ being the nearest neighbors and } \alpha \neq \beta, \\ V_{\mathrm{nnn}} & \text{for } i,j \text{ being the next-nearest neighbors and } \alpha = \beta, \\ 0 & \text{otherwise.} \end{cases} \tag{2}$$

In our notation, negative values of V mean attractive interactions. In the BdG formalism, the Hamiltonian in Eq. (1) can be written in a matrix form

$$H = C^{\dagger} M C,$$

$$C^{\dagger} = (c^{\dagger}_{11\uparrow}, c_{11\downarrow}, c^{\dagger}_{12\uparrow}, c_{12\downarrow}, c^{\dagger}_{21\uparrow}, c_{21\downarrow}, c^{\dagger}_{22\uparrow}, c_{22\downarrow}, \ldots), \tag{3}$$

where M is a $(4N_xN_y)\times(4N_xN_y)$ matrix, with N_x and N_y being the number of lattice sites along $\mathbf{e}_x$ and $\mathbf{e}_y$ directions in the square lattice, respectively. By applying a unitary transformation $Q(Q^{\dagger}Q=I)$, M can be diagonalized as $M=QDQ^{\dagger}$, with $D_{mn}=\delta_{mn}E_m$, where E_m are the eigenvalues of M. The Hamiltonian can be re-expressed in the Bogoliubov quasiparticle representation as

$$H = \gamma^{\dagger} D \gamma,$$

$$C^{\dagger} = \gamma^{\dagger} Q^{\dagger}. \tag{4}$$

In terms of the Bogoliubov quasiparticles, one can recompute the pairing order parameters in Eq. (1) as

$$\begin{aligned} \Delta_{ij,\alpha\beta} &= V_{ij,\alpha\beta}\langle c_{j\beta\downarrow} c_{i\alpha\uparrow}\rangle \\ &= V_{ij,\alpha\beta} \sum_{kl=1}^{4N_xN_y} Q^{\dagger}_{km} Q_{nl} \langle \gamma^{\dagger}_k \gamma_l \rangle \\ &= V_{ij,\alpha\beta} \sum_{l=1}^{4N_xN_y} Q^{*}_{ml} Q_{nl} f(E_l) \\ &= \Delta^{*}_{ji,\beta\alpha}, \end{aligned}$$

$$n = 4(i_y + N_y \times i_x) + 2\alpha - 1,$$

$$m = 4(j_y + N_y \times j_x) + 2\beta, \tag{5}$$

where $f(E_l)$ is the Fermi distribution function, $\mathbf{R}_i=(i_x,i_y)$ is the two-dimensional lattice site vector where i_x and i_y are both integers and $i_x=0,1,\ldots,N_x-1$ $(i_y=0,1,\ldots,N_y-1)$. Here we have set the lattice constant $a=1$. The main procedure of the self-consistent calculation is given below: first start with a set of random complex numbers to every $\Delta_{ij,\alpha\beta}$ in Eq. (3) (that is, we allow time-reversal-symmetry-breaking superconducting order parameters), the Hamiltonian is numerically diagonalized and the unitary transformation Q is obtained by using Eq. (4), then the set of pairing order parameters $\Delta_{ij,\alpha\beta}$ is computed by Eq. (5) for the next iteration step. The calculation is repeated until the absolute error of the order parameters between two consecutive iteration steps is less than 10^{-5}. In the following calculation, we set $N_x=N_y=20$ and $N=N_xN_y$, the chemical potential $\mu=1.6$ corresponds to electron doping. The temperature is set to be $T=0$ K. The hopping integrals are $t_1=-1$, $t_2=1.3$, and $t_3=t_4=-0.85$. Throughout the paper, the energies are measured in units of $|t_1|$.[11] By choosing these hopping parameters, this minimal two-orbital model can exhibit a Fermi surface similar to that obtained from band-structure calculations[14,16,37,38] and contains the essential low-energy physics of iron pnictide superconductors.[11]

III. RESULTS AND DISCUSSION

First by varying the values of V_{nn} and V_{nnn}, we get the phase diagram of the pairing symmetry. The results are

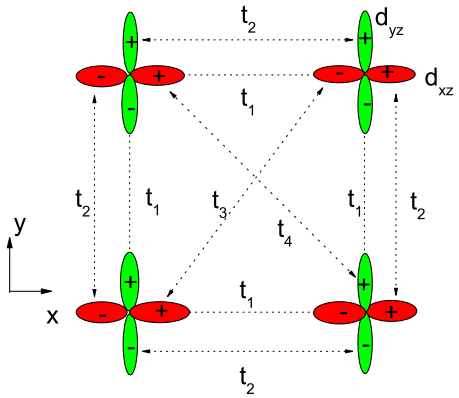

FIG. 1. (Color online) Schematic illustration of the hopping parameters of the two-orbital d_{xz}, d_{yz} model on a square lattice. The projections of the d_{xz} (d_{yz}) orbitals onto the xy plane are depicted in red (green). Here t_1 represents the nearest-neighbor hopping integral between σ orbitals and t_2 the nearest-neighbor hopping integral between π orbitals; t_3 denotes next-nearest-neighbor hopping between similar orbitals and t_4 the next-nearest-neighbor hopping integral between different orbitals.

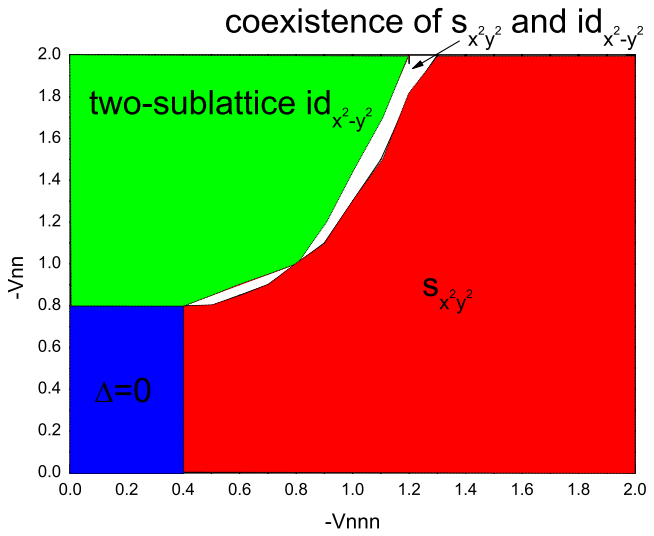

FIG. 2. (Color online) The phase diagram of the pairing symmetry.

shown in Fig. 2. As one can see, on the right red side, there exists only next-nearest-neighbor intraorbital pairing and the pairing order parameters fulfill

$$\Delta_{j\pm\mathbf{e}_x\pm\mathbf{e}_y j,\beta\beta}=\frac{\Delta_0}{4} \tag{6}$$

with $\beta=1,2$ and Δ_0 being real, so the pairing symmetry is $s_{x^2y^2}\sim\cos k_x\cos k_y$. The magnitude of nearest-neighbor interorbital pairing order parameter is always smaller than 10^{-5} in this region. On the other hand, on the upper left green side, the magnitude of next-nearest-neighbor intraorbital pairing order parameter is smaller than 10^{-5} while nearest-neighbor interorbital pairing is dominant. Interestingly, in this region, the order parameter breaks the time-reversal symmetry, with a negligible real part compared to its imaginary part. For a given site j and orbital index β, we have

$$\Delta_{j\pm\mathbf{e}_y j,\bar{\beta}\beta}=-\Delta_{j\pm\mathbf{e}_x j,\bar{\beta}\beta}=-\Delta^*_{j\pm\mathbf{e}_y j,\beta\bar{\beta}}=\Delta^*_{j\pm\mathbf{e}_x j,\beta\bar{\beta}} \tag{7}$$

with $\beta=1,2$. Together with Eq. (5), the order parameter satisfies

$$\Delta_{jj\pm\mathbf{e}_y,\bar{\beta}\beta}=-\Delta^*_{jj\pm\mathbf{e}_y,\beta\bar{\beta}}=-\Delta_{j\pm\mathbf{e}_y j,\bar{\beta}\beta}. \tag{8}$$

Therefore, from Eqs. (7) and (8), we can see that the order parameter has $d_{x^2-y^2}\sim\cos k_x-\cos k_y$ symmetry and if we further define d-wave superconductivity (DSC) order parameter at each site j as

$$\Delta^d_{j,\bar{\beta}\beta}=\frac{\Delta_{j+\mathbf{e}_x j,\bar{\beta}\beta}+\Delta_{j-\mathbf{e}_x j,\bar{\beta}\beta}-\Delta_{j+\mathbf{e}_y j,\bar{\beta}\beta}-\Delta_{j-\mathbf{e}_y j,\bar{\beta}\beta}}{4}, \tag{9}$$

it will form two intersecting sublattices with a relative phase of π (as illustrated in Fig. 3). That is, there is a spontaneous pairing inhomogeneity in real space, which has never been reported before for the iron pnictides. In the following, we will refer to this type of pairing symmetry as two-sublattice $id_{x^2-y^2}$. In the blue region of the phase diagram, the magnitude of both next-nearest-neighbor intraorbital and nearest-neighbor interorbital pairing order parameters is smaller than 10^{-5}, so there is no pairing at all. At last, in the white regions, the pairing symmetry is mainly $s_{x^2y^2}$ with a small amount of two-sublattice $id_{x^2-y^2}$.

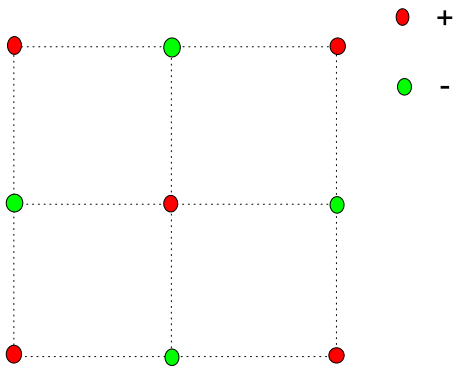

FIG. 3. (Color online) The value of $\Delta^d_{j,\beta\beta}$ at each lattice site. At the red sites, $\Delta^d_{j,\bar{\beta}\beta}$ is positive while at the green sites, it is negative.

In Refs. 28–30, where the pairing symmetries are studied by using the Lanczos method on small clusters with on-site Coulomb interactions in a different two-orbital model, it is shown that at large values of the Hubbard repulsion U, next-nearest-neighbor intraorbital pairing prevails and the pairing symmetry is $s_{x^2y^2}$, consistent with our results. But for nearest-neighbor interorbital pairing only ($V_{\mathrm{nnn}}=0$, $V_{\mathrm{nn}}\neq 0$), we could not find $s_{x^2+y^2}\sim\cos k_x+\cos k_y$ pairing symmetry in our phase diagram, while in Refs. 28–30, it dominates in the phase diagram at intermediate values of the Hubbard repulsion U. We have checked our result by using two different sets of initial $\Delta_{ij,\alpha\beta}$ in the self-consistent calculation, one has every $\Delta_{ij,\alpha\beta}$ being a different random complex number while the other one has all the $\Delta_{ij,\alpha\beta}=x$, with x being an arbitrary real number, thus fulfilling $s_{x^2+y^2}$ symmetry at the very beginning. It turns out that no matter what the initial values of $\Delta_{ij,\alpha\beta}$ are, the converged solution is always two-sublattice $id_{x^2-y^2}$ (complex initial values) or two-sublattice $d_{x^2-y^2}$ (real initial values). These two patterns are degenerate in energy, with a global phase of $\frac{\pi}{2}$ between them, which will not affect the physical consequences discussed below. Therefore, without loss of generality, we restrict our discussion below to the two-sublattice $d_{x^2-y^2}$ case.

Having obtained the possible pairing symmetries in real space since the $s_{x^2y^2}$ pairing symmetry has been extensively discussed elsewhere,[16,17,22,34] we then concentrate on the two-sublattice $d_{x^2-y^2}$ pairing symmetry and transform Eq. (1) into momentum space to see its physical consequences. Since the DSC order parameter in Eq. (9) forms two intersecting sublattices with a relative phase of π, it can be rewritten as

$$\Delta^d_{j,\bar{\beta}\beta}=e^{i\mathbf{Q}\cdot\mathbf{R}_j}\frac{\Delta_0}{4} \tag{10}$$

with $\mathbf{Q}=(\pi,\pi)$ and Δ_0 being real. In momentum space, H_Δ in Eq. (1) is transformed into

$$H_\Delta = \sum_{\mathbf{k},\alpha} (\Delta_{\mathbf{k}} c^\dagger_{\mathbf{k}\alpha\uparrow} c^\dagger_{-(\mathbf{k}+\mathbf{Q})\bar{\alpha}\downarrow} + \text{H.c.}), \tag{11}$$

where

$$\Delta_{\mathbf{k}} = \frac{\Delta_0}{2}(\cos k_x - \cos k_y) \tag{12}$$

with

$$\Delta_0 = \frac{2V_{\text{nn}}}{N} \sum_{\mathbf{k}} (\cos k_x - \cos k_y) \langle c_{\mathbf{k}\alpha\uparrow} c_{-(\mathbf{k}+\mathbf{Q})\bar{\alpha}\downarrow} \rangle. \tag{13}$$

In order to obtain the desired resolution to resolve the resonance in energy, in the following, we set $N=2048\times 2048$. Equations (11) and (12) are just the η pairing proposed by Yang,[35] with nonzero momenta of Cooper pairs. While the η pairing has been studied in some high-temperature superconductors such as the cuprates[31–33] and in a three-orbital model for the iron pnictides where exact diagonalization studies do not favor such a kind of pairing,[39] our calculation reveals the possible η pairing in the iron pnictides. Besides, in Refs. 31–33, a spatially modulated pairing interaction is required to achieve η pairing, our model can yield η pairing spontaneously from a spatially homogeneous pairing interaction V_{nn}.

In momentum space, the Hamiltonian can be written in a matrix form

$$H = \sum_{\mathbf{k}} \psi^\dagger_{\mathbf{k}} M_{\mathbf{k}} \psi_{\mathbf{k}} \tag{14}$$

with

$$\psi^\dagger_{\mathbf{k}} = (c^\dagger_{\mathbf{k}1\uparrow}, c^\dagger_{\mathbf{k}2\uparrow}, c_{-(\mathbf{k}+\mathbf{Q})1\downarrow}, c_{-(\mathbf{k}+\mathbf{Q})2\downarrow}), \tag{15}$$

$$M_{\mathbf{k}} = \begin{pmatrix} \varepsilon_x(\mathbf{k}) - \mu & \varepsilon_{xy}(\mathbf{k}) & 0 & \Delta_{\mathbf{k}} \\ \varepsilon_{xy}(\mathbf{k}) & \varepsilon_y(\mathbf{k}) - \mu & \Delta_{\mathbf{k}} & 0 \\ 0 & \Delta^*_{\mathbf{k}} & -\varepsilon_x(\mathbf{k}+\mathbf{Q}) + \mu & -\varepsilon_{xy}(\mathbf{k}+\mathbf{Q}) \\ \Delta^*_{\mathbf{k}} & 0 & -\varepsilon_{xy}(\mathbf{k}+\mathbf{Q}) & -\varepsilon_y(\mathbf{k}+\mathbf{Q}) + \mu \end{pmatrix}, \tag{16}$$

$$\varepsilon_x(\mathbf{k}) = -2t_1 \cos k_x - 2t_2 \cos k_y - 4t_3 \cos k_x \cos k_y,$$

$$\varepsilon_y(\mathbf{k}) = -2t_2 \cos k_x - 2t_1 \cos k_y - 4t_3 \cos k_x \cos k_y,$$

$$\varepsilon_{xy}(\mathbf{k}) = -4t_4 \sin k_x \sin k_y. \tag{17}$$

Following the standard procedure as described in Refs. 26 and 29, we can diagonalize the tight-binding part of the Hamiltonian and transform it into the band representation as

$$H = \sum_{\mathbf{k}} \varphi^\dagger_{\mathbf{k}} M'_{\mathbf{k}} \varphi_{\mathbf{k}}, \tag{18}$$

where

$$\varphi^\dagger_{\mathbf{k}} = (c^\dagger_{\mathbf{k}+\uparrow}, c^\dagger_{\mathbf{k}-\uparrow}, c_{-(\mathbf{k}+\mathbf{Q})-\downarrow}, c_{-(\mathbf{k}+\mathbf{Q})+\downarrow}),$$

$$M'_{\mathbf{k}} = \begin{pmatrix} E_+(\mathbf{k}) & 0 & 0 & \Delta'_{\mathbf{k}} \\ 0 & E_-(\mathbf{k}) & -\Delta'_{\mathbf{k}} & 0 \\ 0 & -\Delta'^*_{\mathbf{k}} & -E_-(\mathbf{k}+\mathbf{Q}) & 0 \\ \Delta'^*_{\mathbf{k}} & 0 & 0 & -E_+(\mathbf{k}+\mathbf{Q}) \end{pmatrix}, \tag{19}$$

and

$$\varepsilon_\pm(\mathbf{k}) = \frac{\varepsilon_x(\mathbf{k}) \pm \varepsilon_y(\mathbf{k})}{2},$$

$$E_\pm(\mathbf{k}) = \varepsilon_+(\mathbf{k}) \pm \sqrt{\varepsilon^2_-(\mathbf{k}) + \varepsilon^2_{xy}(\mathbf{k})} - \mu,$$

$$\Delta'_{\mathbf{k}} = \text{sgn}[\varepsilon_{xy}(\mathbf{k})]\Delta_{\mathbf{k}}. \tag{20}$$

Here we have used relations $\varepsilon_{xy}(\mathbf{k}+\mathbf{Q})=\varepsilon_{xy}(\mathbf{k})$ and $\varepsilon_-(\mathbf{k}+\mathbf{Q})=-\varepsilon_-(\mathbf{k})$. From Eq. (19), we can see that, although the pairing is interorbital, it still corresponds to the intraband pairing. The Cooper pairs are composed of two electrons [$\mathbf{k}\uparrow$ and $-(\mathbf{k}+\mathbf{Q})\downarrow$] in the same band.

The eigenvalues of $M'_{\mathbf{k}}$ are the energies of quasiparticles, they are

$$\lambda_{1(2)\mathbf{k}} = \mathcal{Z}_+(\mathbf{k}) \mp \sqrt{\mathcal{Q}^2_+(\mathbf{k}) + |\Delta_{\mathbf{k}}|^2}, \tag{21a}$$

$$\lambda_{3(4)\mathbf{k}} = \mathcal{Z}_-(\mathbf{k}) \mp \sqrt{\mathcal{Q}^2_-(\mathbf{k}) + |\Delta_{\mathbf{k}}|^2}, \tag{21b}$$

where $\mathcal{Z}_\pm = [E_\pm(\mathbf{k}) - E_\pm(\mathbf{k}+\mathbf{Q})]/2$ and $\mathcal{Q}_\pm = [E_\pm(\mathbf{k}) + E_\pm(\mathbf{k}+\mathbf{Q})]/2$. Now there no longer exists the symmetry relation of $\lambda_{1\mathbf{k}}=-\lambda_{2\mathbf{k}}$ nor $\lambda_{3\mathbf{k}}=-\lambda_{4\mathbf{k}}$ as in the case of $\mathbf{Q}=(0,0)$. For the two-orbital model, the mean-field superconducting Green's function matrix can be written as

$$g(\mathbf{k},\tau) = -\langle T_\tau \psi_{\mathbf{k}}(\tau) \psi^\dagger_{\mathbf{k}}(0) \rangle \tag{22}$$

and

$$g(\mathbf{k},ip_n)=A_{\mathbf{k}}\begin{pmatrix}\frac{1}{ip_n-\lambda_{1\mathbf{k}}} & 0 & 0 & 0\\ 0 & \frac{1}{ip_n-\lambda_{2\mathbf{k}}} & 0 & 0\\ 0 & 0 & \frac{1}{ip_n-\lambda_{3\mathbf{k}}} & 0\\ 0 & 0 & 0 & \frac{1}{ip_n-\lambda_{4\mathbf{k}}}\end{pmatrix}A_{\mathbf{k}}^{\dagger}, \tag{23}$$

where $A_{\mathbf{k}}$ is a unitary matrix that satisfies

$$A_{\mathbf{k}}^{\dagger}M_{\mathbf{k}}A_{\mathbf{k}}=\begin{pmatrix}\lambda_{1\mathbf{k}} & 0 & 0 & 0\\ 0 & \lambda_{2\mathbf{k}} & 0 & 0\\ 0 & 0 & \lambda_{3\mathbf{k}} & 0\\ 0 & 0 & 0 & \lambda_{4\mathbf{k}}\end{pmatrix}. \tag{24}$$

In the following, we present physical consequences of this type of pairing and compare them with some current experiments. First we study the spin susceptibility defined as $\chi_{zz}(\mathbf{q},i\omega_n)=\Sigma_{\alpha\beta=1}^{2}\chi_{zz}^{\alpha\beta}(\mathbf{q},i\omega_n)$,[11,25] where

$$\chi_{zz}^{\alpha\beta}(\mathbf{q},i\omega_n)=\frac{1}{N}\int_0^{\beta}d\tau e^{i\omega_n\tau}\langle T_{\tau}S_z^{\alpha}(\mathbf{q},\tau)S_z^{\beta}(-\mathbf{q},0)\rangle \tag{25}$$

and

$$S_z^{\alpha}(\mathbf{q},\tau)=\frac{1}{2}\sum_{\mathbf{k}}[c_{\mathbf{k}\alpha\uparrow}^{\dagger}(\tau)c_{\mathbf{k}+\mathbf{q}\alpha\uparrow}(\tau)-c_{\mathbf{k}\alpha\downarrow}^{\dagger}(\tau)c_{\mathbf{k}+\mathbf{q}\alpha\downarrow}(\tau)]. \tag{26}$$

The mean-field spin susceptibility is

$$\chi_{zz}^{\alpha\beta(0)}(\mathbf{q},i\omega_n)=\frac{1}{4}(P_{\beta\alpha}^{(1)}+P_{\beta+2\alpha+2}^{(1)}+P_{\beta+2\alpha}^{(1)}+P_{\beta\alpha+2}^{(1)}), \tag{27}$$

$$P_{ij}^{(1)}(\mathbf{q},i\omega_n)=-\frac{1}{\beta N}\sum_{\mathbf{k}p_n}g_{ij}(\mathbf{k},ip_n)g_{ji}(\mathbf{k}+\mathbf{q},ip_n+i\omega_n)=-\frac{1}{N}\sum_{\mathbf{k}}\sum_{mn=1}^{4}A_{\mathbf{k}im}A_{\mathbf{k}jm}^{*}A_{\mathbf{k}+\mathbf{q}jn}A_{\mathbf{k}+\mathbf{q}in}^{*}\frac{f(\lambda_{m\mathbf{k}})-f(\lambda_{n\mathbf{k}+\mathbf{q}})}{i\omega_n+\lambda_{m\mathbf{k}}-\lambda_{n\mathbf{k}+\mathbf{q}}}. \tag{28}$$

We then use the random-phase approximation (RPA) to take into account the effect of the on-site intraorbital and interorbital Coulomb interactions U and U', respectively. Since the interorbital Coulomb interaction U' does not contribute to the RPA response when only the spin fluctuations are considered,[11,22,25] the RPA spin susceptibility is determined by the matrix equation

$$\chi_{zz}^{\mathrm{RPA}}(\mathbf{q},i\omega_n)=\sum_{\alpha\beta}\{\chi_{zz}^{(0)}(\mathbf{q},i\omega_n)[I-\Gamma\chi_{zz}^{(0)}(\mathbf{q},i\omega_n)]^{-1}\}_{\alpha\beta}, \tag{29}$$

where I is a 2×2 unit matrix and the interaction vertex is $\Gamma=2UI$.

Figure 4 presents the imaginary part of the RPA spin susceptibility $\chi_{zz}^{\mathrm{RPA}}(\mathbf{q},\omega)$ at $\mathbf{q}=(\pi,0)$ as a function of ω, by changing $i\omega_n$ to $\omega+i\eta$ in Eq. (29), for two different Δ_0. As we can see, for $\Delta_0=0.156$, there is an enhancement of intensity around $\omega=0.23$ ($\approx1.5\Delta_0$), suggesting a spin resonance at this energy transfer. However, in contrast to the neutron-scattering experiments,[40–46] no spin gap exists below the resonance energy, which suggests that $\mathbf{q}=(\pi,0)$ wave vector connects two zero energy states (gapless) on the hole and the electron parts of the Fermi surface, respectively. On the other hand, for $\Delta_0=0.28$, the spin response shows some agreement with the experimental observation:[40–46] a spin gap develops at low energy (below $\omega=0.1$) and the weight is transferred to form a spin resonance at about $\omega=0.35$ ($\approx1.25\Delta_0$). This means in our interorbital pairing model, the spin response is dependent on the value of Δ_0 and does not have a generic feature.

In order to better understand its physical consequences, we then proceed to calculate the DOS. The DOS is given by

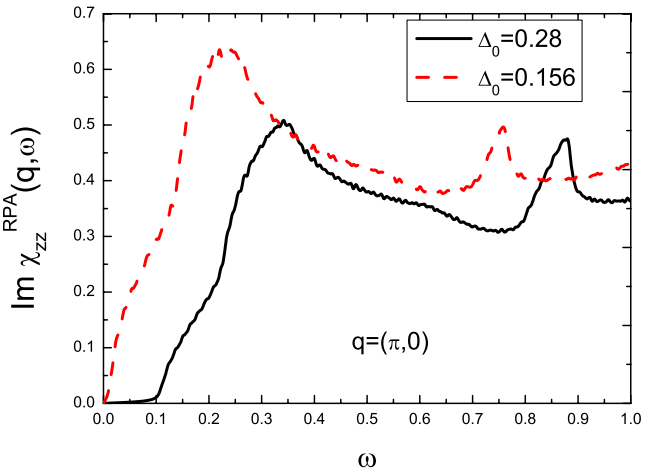

FIG. 4. (Color online) The imaginary part of the RPA spin susceptibility $\chi_{zz}^{\mathrm{RPA}}(\mathbf{q},\omega)$ at $\mathbf{q}=(\pi,0)$ as a function of ω, by changing $i\omega_n$ to $\omega+i\eta$ in Eq. (29), for $\Delta_0=0.28$ (black solid) and $\Delta_0=0.156$ (red dash). We use $\eta=0.004$, $U=3.12$, and $N=2048\times 2048$.

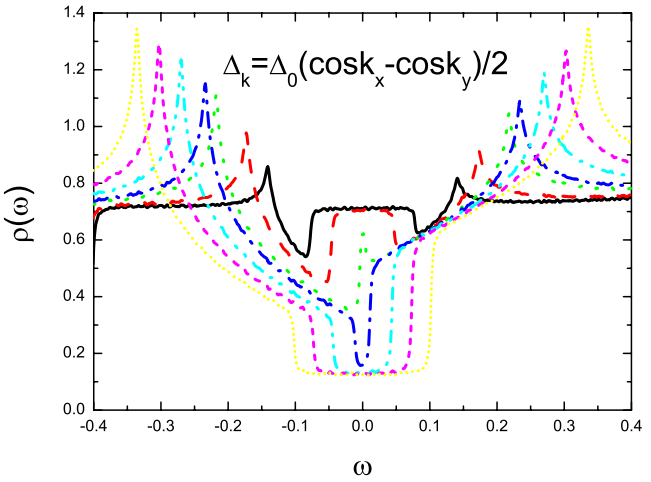

FIG. 5. (Color online) The DOS for various values of Δ_0. $\Delta_0=0.04$ (black solid), 0.08 (red dash), 0.136 (green dot), 0.156 (blue dash dot), 0.2 (cyan dash dot), 0.24 (magenta short dash), and 0.28 (yellow short dot).

$$\rho(\omega) = -\frac{1}{\pi N}\sum_{i,\alpha,\sigma}\mathrm{Im}\langle\langle c_{i\alpha\sigma}|c_{i\alpha\sigma}^{\dagger}\rangle\rangle_{\omega+i\eta}$$

$$= -\frac{1}{\pi N}\sum_{\mathbf{k},\alpha,\sigma}\mathrm{Im}\langle\langle c_{\mathbf{k}\alpha\sigma}|c_{\mathbf{k}\alpha\sigma}^{\dagger}\rangle\rangle_{\omega+i\eta}$$

$$= \frac{1}{N}\sum_{\mathbf{k},\alpha,n}\left[|A_{\mathbf{k}\alpha n}|^2\delta(\omega-\lambda_{n\mathbf{k}}) + |A_{\mathbf{k}\alpha+2n}|^2\delta(\omega+\lambda_{n\mathbf{k}})\right]$$

$$= \frac{\epsilon}{\pi N}\sum_{\mathbf{k},\alpha,n}^{4}\left[\frac{|A_{\mathbf{k}\alpha n}|^2}{\epsilon^2+(\omega-\lambda_{n\mathbf{k}})^2} + \frac{|A_{\mathbf{k}\alpha+2n}|^2}{\epsilon^2+(\omega+\lambda_{n\mathbf{k}})^2}\right]. \quad (30)$$

Here $\mathrm{Im}\langle\langle\cdots\rangle\rangle_{\omega+i\eta}$ is the imaginary part of the retarded Green's function and the Dirac delta function is approximated by

$$\delta(x) \to \frac{\epsilon}{\epsilon^2+x^2} \quad (31)$$

with $\epsilon=0.002$ being chosen. The results are shown in Fig. 5. The density of states shows different behavior depending on the values of Δ_0. For small Δ_0, there is a plateau like an inverse U around $\omega=0$. As Δ_0 increases, the width and height of the plateau decreases and gradually it resembles an inverse V. As Δ_0 increases further, a dip around $\omega=0$ emerges, at first it is V shaped, gradually it becomes U shaped, with an increasing width. The density of states at $\omega=0$ is always nonzero, indicating there are points in the Brillouin zone where the energies of the quasiparticles are zero. There are peaks in the density of states, whose positions are symmetric with respect to $\omega=0$ but the height of the left peak is slightly higher than that of the right one. In addition, there is also some asymmetry near $\omega=0$. In most scanning tunnel microscope experiments,[47–50] the peak positions are symmetric and with a V-shaped gap. The former is consistent with our calculation while the shape of the gap shows some discrepancy.

The finite DOS at the Fermi energy ($\omega=0$) can be understood in this way: based on the expression for the energies of quasiparticles in Eq. (21), we find, on the hole sheets of the Fermi surface located at Γ and M, where $E_-(\mathbf{k})=0$, if $|E_-(\mathbf{k}+\mathbf{Q})|\gg|\Delta_{\mathbf{k}}|$, then either $\lambda_{3\mathbf{k}}$ or $\lambda_{4\mathbf{k}}$ will approach zero. The situation is similar for the electron sheet of the Fermi surface located at X where $E_+(\mathbf{k})=0$, $|E_+(\mathbf{k}+\mathbf{Q})|\gg|\Delta_{\mathbf{k}}|$ will lead to either $\lambda_{1\mathbf{k}}$ or $\lambda_{2\mathbf{k}}$ being close to zero. This is indeed the situation occurring in our two-orbital model. The two hole sheets of the Fermi surface located at Γ and M are not perfectly connected by wave vector $\mathbf{Q}=(\pi,\pi)$, so on those parts of the Fermi surface, where $E_-(\mathbf{k})=0$, we must have $|E_-(\mathbf{k}+\mathbf{Q})|>0$, otherwise they will be nested. On the other hand, according to Eq. (12), $|\Delta_{\mathbf{k}}|\approx 0$ since $\mathbf{k}\approx(0,0)$ (Γ) or $\mathbf{k}\approx(\pm\pi,\pm\pi)$ (M). Therefore, on the hole sheets of the Fermi surface, there is always $\lambda_{3\mathbf{k}}\approx 0$ or $\lambda_{4\mathbf{k}}\approx 0$. The situation is a little different on the electron parts of the Fermi surface located at X. In this case, $|\Delta_{\mathbf{k}}|\approx\frac{\Delta_0}{2}$ since $\mathbf{k}\approx(\pm\pi,0)$ or $\mathbf{k}\approx(0,\pm\pi)$, so there is a critical value of Δ_0, below which we have $\lambda_{1\mathbf{k}}\approx 0$ or $\lambda_{2\mathbf{k}}\approx 0$. For small Δ_0, the energies of quasiparticles on both the electron and the hole parts of the Fermi surface are close to zero, thus contributing to the DOS at $\omega=0$. As Δ_0 increases, the energies of quasiparticles on the electron parts of the Fermi surface are lifted above zero while those on the hole parts of the Fermi surface are still close to zero, so the DOS at $\omega=0$ decreases but still remains finite. This also explains why for small Δ_0, there is no spin gap in the spin susceptibility while a spin gap develops for larger Δ_0.

On the other hand, at large Δ_0, the gap is U shaped, inconsistent with the V-shaped gap observed experimentally.[47–50] One possible reason is that we used a mean-field approximation while similar to the cuprates, when the order-parameter fluctuations are taken into account, one can expect some kind of pseudogap, which typically results in a V-shaped gap in the $d_{x^2-y^2}$ case.[51,52]

IV. CONCLUSION

In conclusion, we have studied a minimal two-orbital model of iron pnictide superconductors. Based on the real-

space BdG equations, we have determined the phase diagram of the pairing symmetry when only nearest-neighbor interorbital and next-nearest-neighbor intraorbital pairing interactions are considered. In the phase diagram where next-nearest-neighbor intraorbital pairing dominates, the pairing symmetry is $s_{x^2y^2} \sim \cos k_x \cos k_y$, consistent with that proposed by Mazin[16] but when nearest-neighbor interorbital pairing prevails, we do not find the $s_{x^2+y^2} \sim \cos k_x + \cos k_y$ pairing symmetry as reported in Refs. 28–30, instead, the pairing order parameter forms two sublattices with a relative phase of π and has $d_{x^2-y^2} \sim \cos k_x - \cos k_y$ symmetry. In momentum space, it corresponds to the η pairing proposed by Yang,[35] with nonzero momenta of Cooper pairs. Although the η pairing has been previously studied for the cuprates by using spatially inhomogeneous pairing interactions,[31–33] our calculation reveals the possible spontaneous η pairing based on a spatially homogeneous pairing interaction. A physical consequence of this type of pairing is to give rise to a significant amount of zero energy (gapless) states around the Fermi surface even in the absence of disorder. For small Δ_0, the energies of quasiparticles on both the electron and the hole parts of the Fermi surface are close to zero, thus contributing to the finite DOS at $\omega=0$ and leading to the disappearance of the spin gap in the superconducting spin susceptibility. As Δ_0 increases, the energies of quasiparticles on the electron parts of the Fermi surface are lifted above zero while those on the hole parts of the Fermi surface still remain close to zero, so the DOS at $\omega=0$ decreases but still remains finite and a spin gap develops in the superconducting spin susceptibility.

We notice, as a model calculation, the momentum dependence of the superconducting gap is in stark contrast to existing ARPES experiments where no node was observed on the hole parts of the Fermi surface.[18–20,53] Therefore, based on the available experimental data, the two-sublattice $d_{x^2-y^2}$ pairing symmetry is excluded for the iron pnictides. Furthermore, since the $s_{x^2y^2}$ pairing symmetry originating from next-nearest-neighbor intraorbital pairing agrees more with current experiments,[16,17,22,34] we can estimate that $|V_{\mathrm{nn}}|$ is smaller than $|V_{\mathrm{nnn}}|$ for the iron pnictides. However, whether interorbital pairing is possible in other materials or not still need to be verified by other experiments.

ACKNOWLEDGMENTS

We thank C. S. Ting, Y. Chen, D. G. Zhang, and T. Zhou for helpful discussions. This work was supported by the Texas Center for Superconductivity and the Robert A. Welch Foundation (Grant No. E-1070) (Y.G. and W.P.S), and by U.S. DOE at LANL under Contract No. DE-AC52-06NA25396 (J.X.Z.)

*Corresponding author; flygaoonly@gmail.com

[1] Y. Kamihara, H. Hiramatsu, M. Hirano, R. Kawamura, H. Yanagi, T. Kamiya, and H. Hosono, J. Am. Chem. Soc. **128**, 10012 (2006).
[2] Y. Kamihara, T. Watanabe, M. Hirano, and H. Hosono, J. Am. Chem. Soc. **130**, 3296 (2008).
[3] G. F. Chen, Z. Li, G. Li, J. Zhou, D. Wu, J. Dong, W. Z. Hu, P. Zheng, Z. J. Chen, H. Q. Yuan, J. Singleton, J. L. Luo, and N. L. Wang, Phys. Rev. Lett. **101**, 057007 (2008).
[4] X. H. Chen, T. Wu, R. H. Liu, H. Chen, and D. F. Chen, Nature (London) **453**, 761 (2008).
[5] H.-H. Wen, G. Mu, L. Fang, H. Yang, and X. Zhu, EPL **82**, 17009 (2008).
[6] G. F. Chen, Z. Li, D. Wu, G. Li, W. Z. Hu, J. Dong, P. Zheng, J. L. Luo, and N. L. Wang, Phys. Rev. Lett. **100**, 247002 (2008).
[7] C. de la Cruz, Q. Huang, J. W. Lynn, J. Li, W. Ratcliff, II, J. L. Zarestky, H. A. Mook, G. F. Chen, J. L. Luo, N. L. Wang, and P. Dai, Nature (London) **453**, 899 (2008).
[8] J. Dong, H. J. Zhang, G. Xu, Z. Li, G. Li, W. Z. Hu, D. Wu, G. F. Chen, X. Dai, J. L. Luo, Z. Fang, and N. L. Wang, EPL **83**, 27006 (2008).
[9] Y. Chen, J. W. Lynn, J. Li, G. Li, G. F. Chen, J. L. Luo, N. L. Wang, P. Dai, C. de la Cruz, and H. A. Mook, Phys. Rev. B **78**, 064515 (2008).
[10] H.-H. Klauss, H. Luetkens, R. Klingeler, C. Hess, F. J. Litterst, M. Kraken, M. M. Korshunov, I. Eremin, S.-L. Drechsler, R. Khasanov, A. Amato, J. Hamann-Borrero, N. Leps, A. Kondrat, G. Behr, J. Werner, and B. Büchner, Phys. Rev. Lett. **101**, 077005 (2008).
[11] S. Raghu, X.-L. Qi, C.-X. Liu, D. J. Scalapino, and S.-C. Zhang, Phys. Rev. B **77**, 220503(R) (2008).
[12] C. Cao, P. J. Hirschfeld, and H.-P. Cheng, Phys. Rev. B **77**, 220506(R) (2008).
[13] S. Lebègue, Phys. Rev. B **75**, 035110 (2007).
[14] D. J. Singh and M.-H. Du, Phys. Rev. Lett. **100**, 237003 (2008).
[15] L. Boeri, O. V. Dolgov, and A. A. Golubov, Phys. Rev. Lett. **101**, 026403 (2008).
[16] I. I. Mazin, D. J. Singh, M. D. Johannes, and M. H. Du, Phys. Rev. Lett. **101**, 057003 (2008).
[17] K. Kuroki, S. Onari, R. Arita, H. Usui, Y. Tanaka, H. Kontani, and H. Aoki, Phys. Rev. Lett. **101**, 087004 (2008).
[18] H. Ding, P. Richard, K. Nakayama, K. Sugawara, T. Arakane, Y. Sekiba, A. Takayama, S. Souma, T. Sato, T. Takahashi, Z. Wang, X. Dai, Z. Fang, G. F. Chen, J. L. Luo, and N. L. Wang, EPL **83**, 47001 (2008).
[19] K. Nakayama, T. Sato, P. Richard, Y.-M. Xu, Y. Sekiba, S. Souma, G. F. Chen, J. L. Luo, N. L. Wang, H. Ding, and T. Takahashi, EPL **85**, 67002 (2009).
[20] D. V. Evtushinsky, D. S. Inosov, V. B. Zabolotnyy, A. Koitzsch, M. Knupfer, B. Büchner, M. S. Viazovska, G. L. Sun, V. Hinkov, A. V. Boris, C. T. Lin, B. Keimer, A. Varykhalov, A. A. Kordyuk, and S. V. Borisenko, Phys. Rev. B **79**, 054517 (2009).
[21] H. Suhl, B. T. Matthias, and L. R. Walker, Phys. Rev. Lett. **3**, 552 (1959).
[22] M. M. Korshunov and I. Eremin, Phys. Rev. B **78**, 140509(R) (2008).
[23] A. B. Vorontsov, M. G. Vavilov, and A. V. Chubukov, Phys. Rev. B **79**, 060508(R) (2009).

[24] K. Seo, B. A. Bernevig, and J. Hu, Phys. Rev. Lett. **101**, 206404 (2008).
[25] K. Seo, C. Fang, B. A. Bernevig, and J. Hu, Phys. Rev. B **79**, 235207 (2009).
[26] T. A. Maier and D. J. Scalapino, Phys. Rev. B **78**, 020514(R) (2008).
[27] Y. Wan and Q.-H. Wang, EPL **85**, 57007 (2009).
[28] M. Daghofer, A. Moreo, J. A. Riera, E. Arrigoni, D. J. Scalapino, and E. Dagotto, Phys. Rev. Lett. **101**, 237004 (2008).
[29] A. Moreo, M. Daghofer, J. A. Riera, and E. Dagotto, Phys. Rev. B **79**, 134502 (2009).
[30] A. Moreo, M. Daghofer, A. Nicholson, and E. Dagotto, Phys. Rev. B **80**, 104507 (2009).
[31] I. Martin, D. Podolsky, and S. A. Kivelson, Phys. Rev. B **72**, 060502(R) (2005).
[32] G. Alvarez, M. Mayr, A. Moreo, and E. Dagotto, Phys. Rev. B **71**, 014514 (2005).
[33] V. Mishra, P. J. Hirschfeld, and Yu. S. Barash, Phys. Rev. B **78**, 134525 (2008).
[34] D. Parker, O. V. Dolgov, M. M. Korshunov, A. A. Golubov, and I. I. Mazin, Phys. Rev. B **78**, 134524 (2008).
[35] C. N. Yang, Phys. Rev. Lett. **63**, 2144 (1989).
[36] W.-L. You, S.-J. Gu, G.-S. Tian, and H.-Q. Lin, Phys. Rev. B **79**, 014508 (2009).
[37] G. Xu, W. Ming, Y. Yao, X. Dai, S.-C. Zhang, and Z. Fang, EPL **82**, 67002 (2008).
[38] K. Haule, J. H. Shim, and G. Kotliar, Phys. Rev. Lett. **100**, 226402 (2008).
[39] M. Daghofer, A. Nicholson, A. Moreo, and E. Dagotto, Phys. Rev. B **81**, 014511 (2010).
[40] A. D. Christianson, E. A. Goremychkin, R. Osborn, S. Rosenkranz, M. D. Lumsden, C. D. Malliakas, I. S. Todorov, H. Claus, D. Y. Chung, M. G. Kanatzidis, R. I. Bewley, and T. Guidi, Nature (London) **456**, 930 (2008).
[41] M. D. Lumsden, A. D. Christianson, D. Parshall, M. B. Stone, S. E. Nagler, G. J. MacDougall, H. A. Mook, K. Lokshin, T. Egami, D. L. Abernathy, E. A. Goremychkin, R. Osborn, M. A. McGuire, A. S. Sefat, R. Jin, B. C. Sales, and D. Mandrus, Phys. Rev. Lett. **102**, 107005 (2009).
[42] S. Chi, A. Schneidewind, J. Zhao, L. W. Harriger, L. Li, Y. Luo, G. Cao, Z. Xu, M. Loewenhaupt, J. Hu, and P. Dai, Phys. Rev. Lett. **102**, 107006 (2009).
[43] A. D. Christianson, M. D. Lumsden, S. E. Nagler, G. J. MacDougall, M. A. McGuire, A. S. Sefat, R. Jin, B. C. Sales, and D. Mandrus, Phys. Rev. Lett. **103**, 087002 (2009).
[44] J. Zhao, L. Regnault, C. Zhang, M. Wang, Z. Li, F. Zhou, Z. Zhao, and P. Dai, arXiv:0908.0954 (unpublished).
[45] L. W. Harriger, A. Schneidewind, S. Li, J. Zhao, Z. Li, W. Lu, X. Dong, F. Zhou, Z. Zhao, J. Hu, and P. Dai, Phys. Rev. Lett. **103**, 087005 (2009).
[46] D. Inosov, J. Park, P. Bourges, D. Sun, Y. Sidis, A. Schneidewind, K. Hradil, D. Haug, C. Lin, B. Keimer, and V. Hinkov, arXiv:0907.3632 (unpublished).
[47] T. Y. Chen, Z. Tesanovic, R. H. Liu, X. H. Chen, and C. L. Chien, Nature (London) **453**, 1224 (2008).
[48] M. Boyer, K. Chatterjee, W. Wise, G. Chen, J. Luo, N. Wang, and E. Hudson, arXiv:0806.4400 (unpublished).
[49] O. Millo, I. Asulin, O. Yuli, I. Felner, Z.-A. Ren, X.-L. Shen, G.-C. Che, and Z.-X. Zhao, Phys. Rev. B **78**, 092505 (2008).
[50] Y. Yin, M. Zech, T. L. Williams, X. F. Wang, G. Wu, X. H. Chen, and J. E. Hoffman, Phys. Rev. Lett. **102**, 097002 (2009).
[51] Y. Yanase and K. Yamada, Physica C **378-381**, 70 (2002).
[52] J. J. Rodríguez-Núñez, A. A. Schmidt, H. Beck, and M. Valera, J. Phys.: Condens. Matter **18**, 11561 (2006).
[53] T. Kondo, A. F. Santander-Syro, O. Copie, C. Liu, M. E. Tillman, E. D. Mun, J. Schmalian, S. L. Bud'ko, M. A. Tanatar, P. C. Canfield, and A. Kaminski, Phys. Rev. Lett. **101**, 147003 (2008).